FEBS Letters 582 (2008) 2458–2462

Molecular determinants of ammonia and urea conductance in plant aquaporin homologs

Marek Dynowski[a], Maria Mayer[a], Oscar Moran[b], Uwe Ludewig[a,*]

[a] *Zentrum für Molekularbiologie der Pflanzen (ZMBP), Pflanzenphysiologie, Universität Tübingen, Auf der Morgenstelle 1, 72076 Tübingen, Germany*
[b] *Istituto di Biofisica, CNR, Via De Marini, 6, I-16149 Genova, Italy*

Received 16 May 2008; revised 6 June 2008; accepted 6 June 2008

Available online 17 June 2008

Edited by Julian Schroeder

Abstract Aquaporins and/or aquaglyceroporins regulate the permeability of plant membranes to water and small, uncharged molecules. Using molecular simulations with a plant plasma membrane aquaporin tetramer, the residues in the channel constriction region were identified as the crucial determinants of ammonia and urea conductance. The impact of these residues was experimentally verified using AtPIP2;1 pore mutants. Several, but not all, mutants with a NIP-like selectivity filter promoted yeast growth on urea or ammonia as sole sources of nitrogen. TIP-like mutants conducted urea but not NH_3, and a residue without direct contact to the pore lumen was critical for conduction in the mutants.

Keywords: Channel; Molecular dynamics; Nitrogen; *Arabidopsis*

1. Introduction

The permeability of plant membranes to uncharged small solutes, such as urea and NH_3, depends on the presence of channels from the major intrinsic membrane protein family [1,2]. Homologous channels are found in archae, bacteriae and mammals, and molecular determinants for their selectivity have been identified [3]. In higher plants, four major subfamilies have been classified according to their similarity and their subcellular localization pattern: the plasma membrane intrinsic proteins (PIPs), tonoplast intrinsic proteins (TIPs), NOD26-like proteins (NIPs) and small basic intrinsic proteins (SIPs) [4,5]. In the model plant *Arabidopsis*, 35 genes encoding aquaporin homologs have been identified [4].

Aquaporins form homo-tetramers, with each subunit providing a functional channel [4,5]. The two constriction regions include a central highly conserved pair of Asn-Pro-Ala (NPA) residues and the aromatic/Arg (ar/R) region. The latter is located more closely to the extracellular pore exit, is generally the most narrow part of the pore and is critical for water and solute conduction, while the NPA region is involved in the selection against protons [6]. An increasing pore diameter allows the conduction of larger solutes, such as the plant nitrogen fertilizer urea [7]. The urea permeability of plant plasma membranes is generally lower than that of the tonoplast, which correlates with high urea transport rates in some TIPs compared to PIPs [8]. However, a plasma membrane PIP, NtAQP1 from tobacco, has been reported to transport urea, as was AtNIP6.1 [5,7]. Specific residues are required for urea conduction [7].

How aquaporins select between smaller substrates, such as NH_3, which is not substantially larger than water, is less clear [3]. Ammonium is also widely used to fertilize plants and is a by-product of many metabolic processes, including urea degradation [9]. Channel mediated NH_3 conduction has been reported in the plant symbiosome membrane. This envelope separates symbiotic bacteria from plant cells and is rich in the aquaporin homolog nodulin 26 (NOD26) [10,11]. In addition, homologs of the TIP2 family conduct ammonia [1,2] and specific pore mutations abolish flux [1]. However, the importance of the channel pores for ammonia conductance in TIP2;2 from wheat has been challenged by the finding that the conduction of water and ammonia is differentially affected by inhibitors [12].

Molecular dynamics simulations were used to identify the molecular determinants of ammonia conduction in plant aquaporins. The residues at the ar/R constriction region were most critical. These data were used to design a series of mutants in which the crucial – solute conductance determining – residues in AtPIP2;1 were exchanged to TIP and NIP-like residues. Experimental determination of the transport function of pore mutants expressed in yeast confirmed the role of this region on selectivity and allowed the identification of the structural requirements for ammonia and urea conduction.

2. Results

2.1. Simulation of small solute conduction in a plant aquaporin

Most residues that are in direct contact with the pores, especially those of the ar/R constriction region, are strongly conserved among PIP-type aquaporins, including the crystallized plasma membrane aquaporin SoPIP2;1 from spinach [13]. All 13 PIP1- and PIP2-type homologs from *Arabidopsis* contain an identical ar/R filter consisting of phenylalanine (Phe), histidine (His), threonine (Thr) and arginine (Arg). We, therefore, chose SoPIP2;1 as a representative model to simulate the conduction mechanism of ammonia and urea in plant PIP aquaporins. The setup for steered molecular dynamics simulations on the "open" (see Section 4) tetrameric SoPIP2;1 is shown in Fig. 1A. The lipid embedded tetramer was solvated with water,

*Corresponding author. Fax: +49 7071 29 3287.
E-mail address: uwe.ludewig@zmbp.uni-tuebingen.de (U. Ludewig).

0014-5793/$34.00
doi:10.1016/j.febslet.2008.06.012

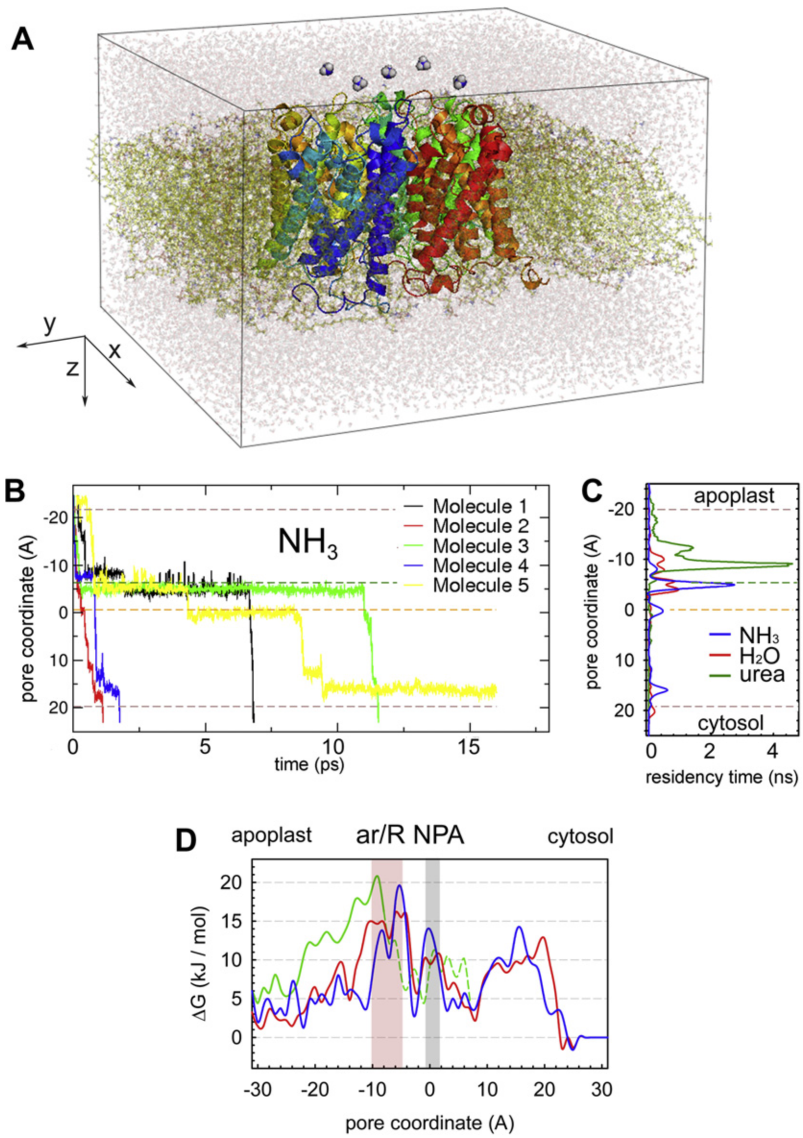

Fig. 1. Simulation of NH_3 transport in a plant aquaporin. (A) Setup of the SoPIP2;1 tetramer embedded in a POPE membrane solvated with water. The starting positions of five NH_3 molecules along the channel axis are explicitly shown. (B) Trajectories of five individual NH_3 molecules crossing the pore. (C) Weighted residency times along the pore axis for water (red), NH_3 (blue) and urea (green). The entrance and exit sites along the channel axis (dashed brown lines), the selectivity filter (ar/R, dashed green line) and the NPA region (dashed yellow line) are indicated. (D) Estimated apparent energy (ΔG^*) profiles along the channel axis deduced from the residency times for NH_3, H_2O and urea.

as has been described [14]. Examples of the trajectories of individual NH_3 molecules along the z-axis are shown in Fig. 1B. Although a steering force was applied to each NH_3 molecule, not every NH_3 entered a pore. However, all the molecules that found their way into a pore vestibule crossed the channel fully. A major site of residency was at the ar/R region, which can be seen in the residency histogram from three independent 16 ns simulations, with a total of 14 NH_3 molecules crossing the pore. Compared to water, NH_3 crossed the pore less rapidly, while urea conduction was impaired (Fig. 1C) [14]. The preferred residency sites for water and the other solutes partially overlapped.

Apparent energy barriers along the *z*-axis were estimated from the dwell time histograms and are shown in Fig. 1D. Despite a bias caused by the applied forces, ranging from 40 to 46 pN, these trajectories can be compared, since all three substrates were handled equally. The major barrier for NH_3 was at the ar/R region and was ~4 kJ/mol higher than for H_2O, indicating that NH_3 is a less preferred substrate. Likewise, the key barrier for urea conduction was located just in front of the barrier for NH_3 and was estimated to be at least ~5 kJ/mol higher than the barrier for water.

Two of the NH_3 molecules entered the central cavity between the monomer channels and one of these crossed the entire membrane after 16 ns. Another NH_3 passed the membrane lipids, suggesting that pure POPE membranes still let some ammonia through. Taking into account the well-established intrinsic background permeability of lipid membranes to NH_3 [15], it remains questionable whether PIP aquaporins can thus enhance the flux across native membranes (see Section 3).

The simulations showed that the small size of NH_3 did apparently not cause the extended residency time at the selectivity filter. While urea was apparently too large to readily cross the constriction region, the major NH_3 residency peaked slightly further inside the pore. Visual inspection of individual conduction events showed that the high barrier for NH_3 resulted from effects on the water molecules within the pore. While individual waters established a defined array of hydrogen bonds, NH_3 molecules interfered with this property and even caused imperfect arrangement of the surrounding waters. As a result, the formation of a line of waters within the pore – a characteristic of rapid water conduction – was prevented [6].

That the ar/R region is the key determinant of whether NH_3 or urea are conducted in SoPIP2;1 coincides with mutational results (*see below*) and former work, in which residues in the ar/R region were involved in the ammonia [1] or urea conductance [7] in plant aquaporin homologs.

2.2. Solute conduction in PIP2;1 with TIP-like selectivity filter

To investigate the role of the ar/R region on the NH_3 and urea permeability, we experimentally tested a series of mutanted AtPIP2;1. Mutant channels with TIP-like ar/R filters were constructed. Up to four residues from AtPIP2;1 were exchanged to mimic all TIPs from *Arabidopsis*. These TIP-like mutants (TIPL) were expressed in selective yeast strains and cells were grown under selective conditions. The names of the constructs and their respective pore compositions are given in Table 1.

As expected from the molecular simulations, the AtPIP2;1 did not allow sufficient ammonia and urea influx for yeast growth under selective conditions (Fig. 2A and B). In contrast, AtPIP2;1 with ar/R residues exchanged to those encountered in TIP5;1 (TIPL5;1) was capable of transporting urea, as growth tests determined (Fig. 2). Surprisingly, the other mutants with TIP-like ar/R residues did not conduct, or only minimally conducted urea, although native TIP1, TIP2 and TIP4 homologs are known to transport this solute [16] (Fig. 2A).

We, therefore, examined whether the constriction region in SoPIP2;1 and in homology models with exchanged ar/R residues is sufficiently large to accommodate TIP-like amino acid side chains. Interestingly, replacing phenylalanine 87 by a histidine resulted in a blocked pore, because it twisted into the pore lumen (Fig. 2C). This twist was caused by the neighboring Thr side chain at position 55, which has no direct contact with the pore lumen. In all the TIPs, the corresponding residue is a smaller Gly. Therefore the introduced His was combined with Gly at position 55, leading to TIPLG channels (Fig. 2C). These were permeable to urea (Fig. 2). Surprisingly, none of the TIP-like mutants promoted growth on limiting ammonia, suggest-

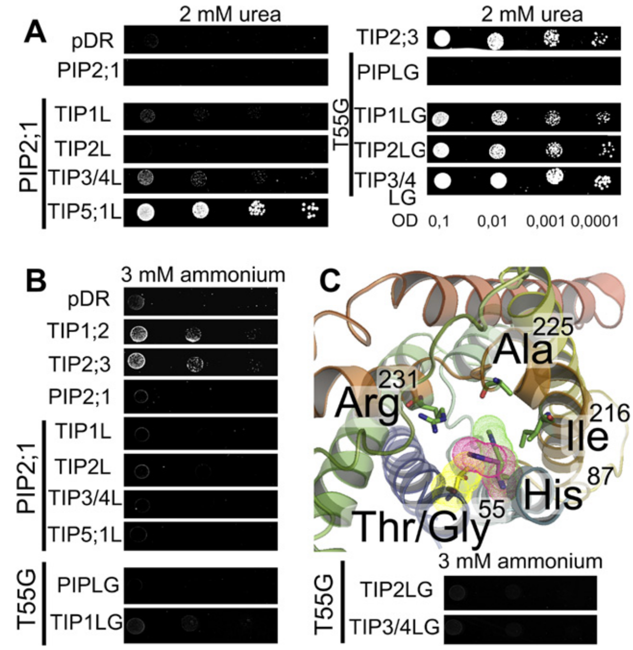

Fig. 2. Transport activity of TIP-like AtPIP2;1 mutants. (A) Growth on urea (2 mM) as sole nitrogen source. (B) Growth on ammonium (3 mM) as sole nitrogen source. Growth improvement by pore mutants of AtPIP2;1 is compared with empty plasmid transformed yeast (pDR), wild-type AtPIP2;1, AtTIP1;2 and AtTIP2;3. Tenfold dilution series are shown, beginning with identical optical density (OD) of 1.0. (C) Top view into the pore of superimposed homology models of TIP2-like pore mutants with and without additional ^{55}Thr to Gly mutation.

Table 1
Amino acid compositions in the constriction region of AtPIP2;1 mimicing different aquaporin isoforms

Construct	Position in PIP2;1					Corresponding MIPs
	55	87	216	225	231	
PIPL	Thr	Phe	His	Thr	Arg	PIP1 subfamily, PIP2-subfamily
PIPLG	Gly	Phe	His	Thr	Arg	
TIP1L	Thr	His	Ile	Ala	Val	
TIP1LG	Gly	His	Ile	Ala	Val	TIP1;1, TIP1;2, TIP1;3
TIP3/4L	Thr	His	Ile	Ala	Arg	
TIP3/4LG	Gly	His	Ile	Ala	Arg	TIP3;1, TIP3;2, TIP4;1
TIP2L	Thr	His	Ile	Gly	Arg	
TIP2LG	Gly	His	Ile	Gly	Arg	TIP2;1, TIP2;2, TIP2;3
TIP5;1L	Ala	Asn	Val	Gly	Cys	TIP5;1
NIP124L	Thr	Trp	Val	Ala	Arg	
NIP124LG	Gly	Trp	Val	Ala	Arg	NIP1;1, NIP1;2, NIP2;1, NIP4;1, NIP4;2
NIP3L	Thr	Trp	Ile	Ala	Arg	
NIP3LG	Gly	Trp	Ile	Ala	Arg	NIP3;1
NIP5;1L	Ala, n.r.	Ala	Ile	Gly	Arg	NIP5;1
NIP6;1L	Gly, n.r.	Ala	Ile	Ala	Arg	NIP6;1
NIP7;1L	Val, n.r.	Ala	Val	Gly	Arg	NIP7;1

n.r., not relevant.

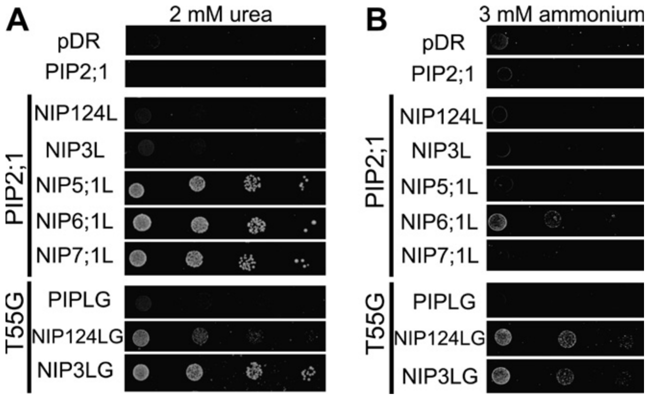

Fig. 3. Transport activity of NIP-like AtPIP2;1 mutants. (A) Growth of the Δ*dur3* yeast strain expressing NIPL pore mutants of AtPIP2;1 on urea (2 mM) as sole nitrogen source. (B) Growth on ammonium (3 mM) as sole nitrogen source. NIPL and NIPLG pore mutants of AtPIP2;1 are compared with empty plasmid transformed yeast (pDR) and wild type AtPIP2;1. Tenfold dilution series are shown, beginning with identical optical density (OD) of 1.0.

ing that a TIP-like selectivity filter is not sufficient to enhance the NH_3 permeability in AtPIP2;1 (Fig. 2).

TIP1 channels have a unique ar/R filter, in which the highly conserved arginine (Arg 231 in SoPIP2;1) is replaced by valine. When compared to Arg-containing TIP2- or TIP3-like mutants, the TIP1-like channels were similar in promoting growth on urea and were identical on ammonia. The difference in the Arg/Val residue is, thus, not critical for ammonia and urea transport.

2.3. Ammonia and urea conduction with NIP-like selectivity filters

The same growth tests were performed with channels that contained NIP-like selectivity filters. NIP-like mutants (NIPL) that correspond to NIP5;1, NIP6;1 and NIP7;1 channels had, among other amino acid changes, Phe 87 replaced by Ala and promoted growth on urea (Fig. 3). In contrast, other NIP-like channels, where Phe 87 was replaced by Trp, show urea transport only when Thr 55 was exchanged to Gly as well, the respective amino acid in native NIPs. In contrast to the TIPL aquaporins, the NIPLG constructs and NIPL6;1 improved growth on ammonia (Fig. 3). The sequences of NIPL6;1 and NIPL5;1 only differ in a single amino acid (Ala/Gly) at position 225, indicating that minor differences affect ammonia conductance.

3. Discussion

The simulations of water and small solute conduction in SoPIP2;1 indicated, that the ar/R region is the major energetic barrier for conduction. Similar results have recently been obtained from simulations on human and bacterial homologs [17]. Although the calculations suggest that NH_3 is conducted in SoPIP2;1 at a low rate, this does not appear to be sufficient to increase the permeability of the lipid membrane to NH_3 (Fig. 2). Lipid membranes, such as POPE membranes, impair NH_3 passage with an intrinsic energy barrier of 19 kJ/mol and a rate limiting major barrier of similar hight was found for NH_3 transport in the human aquaporin AQP1 (18 kJ/mol) [17]. An apparent maximal barrier of 20 kJ/mol was observed for SoPIP2;1, indicating that these aquaporins do not improve ammonia flux. Different simulation techniques (umbrella sampling) and force fields yielded similar maximal barriers [17]. The simulations suggest that the selectivity filter restricts NH_3 passage by preventing the formation of a favorable hydrogen bonding network, as observed in pure water simulations, for example. A similar mechanistic explanation for selectivity against small substrates other than water has been proposed for human AQP1 [17].

In initial preliminary experiments, we noticed that some NIP channels were non-functional in yeast. AtNIP5;1 conducts boron and urea when expressed in *Xenopus* oocytes [18], but AtNIP5;1 caused neither boron sensitivity nor urea uptake in yeast (*data not shown*). Thus, a direct comparison of the selectivity of individual plant aquaporin homologs with distinct ar/R regions will be biased by their expression level, the differential trafficking to the correct membrane and the possible regulation of their open probability [19].

To avoid this bias and to explicitly test the relevance of different selectivity filters, we replaced the potentially crucial – solute conductance determining – residues in AtPIP2;1 only. While the native AtTIP1;2 promoted yeast growth on ammonia, PIP2;1 mutants with an identical TIP-like selectivity filter did not (Fig. 2). This is in agreement with results obtained from previous inhibitor studies [12]. It supports the theory that NH_3 crossed the membrane using the central pore formed by the four monomers and challenges the conclusion that an Arg/His pair in the selectivity filter region accommodates NH_3 conductivity [3]. Interestingly, in one simulation NH_3 crossed the membrane using that central pore. While the simulations suggest that the tetramer center is not a preferential NH_3 pore in SoPIP2;1, however, this may not be the case for other homologs. An advantage of conduction through the tetramer center is that water will not compete with NH_3 conduction through the hydrophobic tetramer center.

The large energy barrier for urea in SoPIP2;1 matches the inability of AtPIP2;1 to promote yeast growth on this substrate. This is in agreement with the low permeability of the plant plasma membrane and with the inability of many PIPs to transport urea. Urea may, however, pass the selectivity filter at low rate [5]. Urea was well conducted by TIPLG channels, which resemble TIP1-, TIP2- and TIP4-type members from *Arabidopsis* [16], but not by TIPL channels. Using homology modelling, we successfully predicted that a Thr/Gly exchange close to the ar/R region is responsible for the differences (Fig. 2C). The results foretell that the pollen-specific AtTIP5;1 will transport large solutes such as urea.

The growth tests confirmed that several native NIPs conduct urea, such as AtNIP6;1 [7] and AtNIP5;1 (*data not shown*). Interestingly, NIP6;1, but not NIP5;1 or NIP7;1 is predicted to transport substantial amounts of ammonia, although these channels have only one minor amino acid difference in the relevant region (Tab.1). NIPLG, but not NIPL channels, promoted growth on ammonia, although these have identical ar/R residues. Not only the ar/R residues per se, but also their orientation and exact position appear to be critical. Channel homologs from lower organisms with completely distinct residues in the ar/R region also conduct ammonia, which hinders a simple, general conclusion on the molecular requirements for efficient ammonia conductance [3]. Furthermore, other channel region may be also of importance. Whether the ammonia and urea conduction by individual aquaporin homologs is found in the native NIP channels and whether this is physiologically relevant must be directly investigated in plants at a future time.

4. Materials and methods

4.1. Plasmid constructs and yeast expression

All the mutants were introduced into the pDR plasmid containing AtPIP2;1 (*At3g53420*) using the Quickchange kit from Stratagene. All constructs were verified by sequencing. Saturated cultures of yeast transformed with the respective constructs were diluted to the same optical density of 1 and were then spotted in 10-fold dilution on control plates (2 mM arginine, *no differences observed*) and plates containing either 2 mM urea or 3 mM ammonia (pH 6.5 with MES) as sole nitrogen source. For growth tests with urea the Δ*dur3* yeast strain was used [20], for those with ammonium a yeast mutant that lacks three endogenous MEP transporters (ΔΔΔ*mep*) was used [21]. Yeast nitrogen base medium (Difco) supplemented with 2% glucose was used and photos were taken after identical incubation times (2–3 days). High contrast scanning was used to optimally visualize even weak growth differences.

4.2. Molecular dynamics simulations

Molecular dynamics simulations (MD) were carried out using the NAMD2 program [22] and the Amber03 force field, on an ''open conformation'' of SoPIP2;1 [14]. Minimization and equilibration preceded simulations, as described [14]. A constant force vector in z-direction was applied to water, NH_3 or urea, to reduce calculation times [23]. The trajectories along the z-axis were calculated relative to the Cα of valine 206. The z-positions of Cα of lysine 144 were taken as external entrance and the positions of the Cα of proline 33 as internal exit, respectively.

4.3. Residency time and apparent energy profiles

The residency histogram along the z-axis was accumulated in 1 Å intervals and the apparent energy profiles were then estimated from transition state theory as

$$\Delta G^{\ddagger *} = -RT \ln\left(\frac{1}{\tau}\frac{h}{Tk_{\mathrm{b}}}\right)$$

where τ is the residence time, $\Delta G^{\ddagger *}$ is the apparent Gibbs free energy of activation, T is the absolute temperature, R is the universal gas constant, k_{b} is Boltzmann's constant, and h is Planck's constant.

Acknowledgements: We thank P. Neumann for excellent technical assistance and F. de Courcy for critically reading the manuscript. This work was partially supported by a grants of the Landesstiftung Baden Württemberg to U.L. Simulations were carried out at the HPC-center of the University of Tübingen and the Scientific Supercomputing Center (SSC) Karlsruhe, Germany.

References

[1] Jahn, T.P., Moller, A.L., Zeuthen, T., Holm, L.M., Klaerke, D.A., Mohsin, B., Kuhlbrandt, W. and Schjoerring, J.K. (2004) Aquaporin homologues in plants and mammals transport ammonia. FEBS Lett. 574, 31–36.

[2] Loqué, D., Ludewig, U., Yuan, L. and von Wiren, N. (2005) Tonoplast aquaporins AtTIP2;1 and AtTIP2;3 facilitate NH3 transport into the vacuole. Plant Physiol. 137, 671–680.

[3] Wu, B. and Beitz, E. (2007) Aquaporins with selectivity for unconventional permeants. Cell Mol. Life Sci. 64, 2413–2421.

[4] Maurel, C. (2007) Plant aquaporins: novel functions and regulation properties. FEBS Lett. 581, 2227–2236.

[5] Kaldenhoff, R. and Fischer, M. (2006) Functional aquaporin diversity in plants. Biochim. Biophys. Acta 1758, 1134–1141.

[6] Tajkhorshid, E., Nollert, P., Jensen, M.O., Miercke, L.J., O'Connell, J., Stroud, R.M. and Schulten, K. (2002) Control of the selectivity of the aquaporin water channel family by global orientational tuning. Science 296, 525–530.

[7] Wallace, I.S. and Roberts, D.M. (2005) Distinct transport selectivity of two structural subclasses of the nodulin-like intrinsic protein family of plant aquaglyceroporin channels. Biochemistry 44, 16826–16834.

[8] Gerbeau, P., Guclu, J., Ripoche, P. and Maurel, C. (1999) Aquaporin Nt-TIPa can account for the high permeability of tobacco cell vacuolar membrane to small neutral solutes. Plant J. 18, 577–587.

[9] Miller, A.J. and Cramer, M.D. (2004) Root nitrogen acquisition and assimilation. Plant Soil 274, 1–36.

[10] Niemietz, C.M. and Tyerman, S.D. (2000) Channel-mediated permeation of ammonia gas through the peribacteroid membrane of soybean nodules. FEBS Lett. 465, 110–114.

[11] Wallace, I.S., Choi, W.G. and Roberts, D.M. (2006) The structure, function and regulation of the nodulin 26-like intrinsic protein family of plant aquaglyceroporins. Biochim. Biophys. Acta 1758, 1165–1175.

[12] Bertl, A. and Kaldenhoff, R. (2007) Function of a separate NH(3)-pore in Aquaporin TIP2;2 from wheat. FEBS Lett. 581, 5413–5417.

[13] Tornroth-Horsefield, S., Wang, Y., Hedfalk, K., Johanson, U., Karlsson, M., Tajkhorshid, E., Neutze, R. and Kjellbom, P. (2006) Structural mechanism of plant aquaporin gating. Nature 439, 688–694.

[14] Dynowski, M., Schaaf, G., Loque, D., Moran, O. and Ludewig, U. (in press) Plant plasma membrane water channels conduct the signaling molecule H2O2. Biochem J, doi:10.1042/BJ2008.287.

[15] Walter, A. and Gutknecht, J. (1986) Permeability of small nonelectrolytes through lipid bilayer membranes. J. Membr. Biol. 90, 207–217.

[16] Liu, L.H., Ludewig, U., Gassert, B., Frommer, W.B. and Von Wiren, N. (2003) Urea transport by nitrogen-regulated tonoplast intrinsic proteins in arabidopsis. Plant Physiol. 133, 1220–1228.

[17] Hub, J.S. and de Groot, B.L. (2008) Mechanism of selectivity in aquaporins and aquaglyceroporins. Proc. Natl. Acad. Sci. USA 105, 1198–1203.

[18] Takano, J., Wada, M., Ludewig, U., Schaaf, G., von Wiren, N. and Fujiwara, T. (2006) The Arabidopsis major intrinsic protein NIP5;1 is essential for efficient boron uptake and plant development under boron limitation. Plant Cell 18, 1498–1509.

[19] Tournaire-Roux, C., Sutka, M., Javot, H., Gout, E., Gerbeau, P., Luu, D.T., Bligny, R. and Maurel, C. (2003) Cytosolic pH regulates root water transport during anoxic stress through gating of aquaporins. Nature 425, 393–397.

[20] Liu, L., Ludewig, U., Frommer, W.B. and von Wiren, N. (2003) AtDUR3 encodes a new type of high-affinity urea/H^+ symporter in *Arabidopsis thaliana*. Plant Cell 15, 790–800.

[21] Marini, A.M., Soussi-Boudekou, S., Vissers, S. and André, B. (1997) A family of ammonium transporters in *Saccharomyces cerevisiae*. Mol. Cell. Biol. 17, 4282–4293.

[22] Phillips, J.C. et al. (2005) Scalable molecular dynamics with NAMD. J. Comput. Chem. 26, 1781–1802.

[23] Jensen, M.O., Park, S., Tajkhorshid, E. and Schulten, K. (2002) Energetics of glycerol conduction through aquaglyceroporin GlpF. Proc. Natl. Acad. Sci. USA 99, 6731–6736.